

Cite this article as: Wang Pengjia, Ma Yuning, Peng Baoying, et al. Effects of Mg on P Segregation at α -Fe $\Sigma 3(111)$ GB[J]. Rare Metal Materials and Engineering, 2025, 54(05): 1156-1164. DOI: <https://doi.org/10.12442/j.issn.1002-185X.20240554>.

ARTICLE

Effects of Mg on P Segregation at α -Fe $\Sigma 3(111)$ GB

Wang Pengjia¹, Ma Yuning¹, Peng Baoying¹, Lin Kun³, Li Xiaobing², Liu Kui²

¹ College of Mechanical and Electrical Engineering, Beijing Information Science and Technology University, Beijing 102206, China; ² Ji Hua Laboratory, Foshan 528200, China; ³ Institute of Solid State Chemistry, University of Science and Technology Beijing, Beijing 100083, China

Abstract: First-principles theory calculations were used to investigate the segregation behavior of P and Mg as well as the interactions between Mg and P at α -Fe $\Sigma 3(111)$ $[1\bar{1}0]$ symmetrical tilt grain boundary (GB). Results demonstrate that both P and Mg are segregated at GB, and P has a stronger segregation potency. Mg prefers to substitute at grain boundary plane with the largest absorbable vacancy, whereas P inclines to substitute at the sites near Fe atoms to form strong covalent Fe-P bonds. When Mg exists at GB, the segregation behavior of P may be greatly inhibited by the decrease in possible solution sites and the increase in segregation energy. P has stronger interactions with Mg at GB, forming a lower energy hybridization peak. These results can be used to explain why the addition of a small amount of Mg can ameliorate the temper embrittlement phenomenon.

Key words: α -Fe; GB; P; Mg; segregation; density functional theory

1 Introduction

Impurities segregated at grain boundaries (GBs) always cause a dramatic decrease in mechanical properties of alloys. One of the most typical results is the temper embrittlement in steels. This kind of embrittlement is usually found in low-alloying steels, such as 2.25Cr-1Mo and Ni-Cr-Mo, during heat treatment or servicing at a critical temperature range (350 – 600 °C) [1–8]. When the temper embrittlement occurs, the fracture characteristics are transformed from a transgranular fracture to an intergranular one by a great decrease in ductility. Meanwhile, the ductile to brittle transition temperature (DBTT) also rises to a higher level [9–11]. Many theories have been proposed to explain this phenomenon and a widely acceptable theory proposes that the solubility of impurity atoms in GB is always much higher than that in the matrix, which induces the dissociative atoms to segregate at GB and causes the decrease in GB strength [12]. According to Ref. [13], combining both basic theoretical calculations and experimental research, the mechanisms behind GB strength decrease caused by impurity atoms include the following effects: (1) atomic size effect, which results from the local strains induced by the solution of oversize atoms [14]; (2) GB decohesion resulting from the formation of low energy

bonds [15–17]; (3) GB decohesion resulting from the formation of covalent bonds, which in turn impairs the original metal bonds [18–19]. It is well acknowledged that GB embrittlement cannot be caused by a sole mechanism but a comprehensive result of a few mechanisms.

Many trace elements (such as P, S, Sb, Sn, Se, and Te) were testified to trigger GB embrittlement. Among these impurities, P is one of the most frequently-used impurities in steels due to its higher chemical composition [20]. According to the related research, P has strong segregation tendency to GB and causes embrittlement in various conditions. Zheng et al [21] pointed out that in 12Cr1MoV steel, P was segregated at GB after aging at 540 °C for 15 h whether it was under the elastic stress or not. Kameda et al [11] emphasized that DBTT shifts of thermally aged or neutron-irradiated A533B steel and 2.25Cr-1Mo were caused by the segregation of P at GB. The effect of P on GB embrittlement was also evaluated by theoretical calculations. Wu et al [22] showed that the embrittlement of P-containing GB can be explained by the bond mobility mechanism. Yuasa et al [19] calculated the P-segregated $\Sigma 3$ GB in body-centered cubic (bcc) Fe. They found that even though P and surrounded Fe atoms formed high charge density covalent Fe-P bonds, the mobility of electrons was greatly reduced, thus affecting the density states of the Fe-Fe bonds and leading to an

Received date: August 27, 2024

Foundation item: National Natural Science Foundation of China (51801210)

Corresponding author: Li Xiaobing, Ph. D., Professor, Ji Hua Laboratory, Foshan 528200, P. R. China, E-mail: lixb@jihualab.ac.cn

Copyright © 2025, Northwest Institute for Nonferrous Metal Research. Published by Science Press. All rights reserved.

embrittlement behavior.

To alleviate the detrimental effect of P in alloys, methods have been applied to either strengthen GB or to eliminate P from GB. For example, Wu et al^[23] discovered that the temper embrittlement susceptibility of medium carbon CrNi3Mo steel could be improved by alloying with Ce. The main reason was the formation of Ce-P compound as well as the contributions of Ce segregation to GB strength. Lu et al^[24] investigated the positive effect of hafnium on controlling the intergranular segregation of P in ferrite steels and ascribed the mechanism to the solute drag model. They showed that hafnium could suppress the segregation of P to about one-sixth of the segregation degree of hafnium-free alloy. Mo is also found to play a significant role in impeding P segregation at GB by forming Mo-P compound in matrix due to the strong interactions between these two atoms. However, this positive effect is greatly hindered when Mo and C are precipitated as carbides during the aging process^[11-25]. Besides, Song^[26] and Hong^[27] et al proved that B is preferentially located at GBs, which can reduce the possible GB segregation sites of P. Heo et al^[28] analyzed the effect of decarburization on a low-alloying steel with 0.019wt% P, and pointed out that a drastic decrease in intergranular fracture strength could be found with the increase in P concentration at GB as a result of decarburization at 900 °C. This result indicated that P was the GB segregation atom, and GB pre-located atom (carbon) might have a great effect to impede the P segregation.

2.25Cr-1Mo with bcc-Fe matrix is one of the main Cr-Mo low-alloying steels widely used in power and petrochemical industries for boiler, piping, and chemical reaction vessels^[10,29]. Currently, a series of experiments were performed on the hindrance effect of Mg on the temper embrittlement induced by P in 2.25Cr-1Mo. This is because Mg is a quite commonly employed element to purify molten steel and modify inclusion in steels, and it also has a positive effect on GB strength of superalloys^[4-5,30-34]. The impact toughness evolution of 2.25Cr-1Mo alloy with 0.056wt% P addition after step-cooling was studied. Through auger electron spectroscopy (AES), it was found that Mg was prone to segregation at GB to decrease the segregation amount of P at GB, and when the content of Mg increases from 0.002wt% to 0.006wt%, the increment of DBTT after step-cooling decreases from 26.57 °C (Mg-free alloy) to 18.45 and 9.30 °C, respectively. Mg is believed to be a brittle-trigger element^[13], but the mechanism of P segregation is still obscure only based on the experimental phenomenon.

In this research, the segregation behavior of Mg at GB of bcc Fe was investigated with the assistance of first-principles calculation. Its effect on the solution behavior of P at GB was also studied. This research provided new insights into Mg segregation behavior at GB in bcc Fe, and also clarified the element interactions of Mg and P at GB, guiding the element addition and alloy design.

2 Computational Details and GB Models

Vienna ab initio simulation package^[35-37] was used with the

projector augmented wave potential for the ion-electron interaction^[38-39]. An energy cutoff of 400 eV was chosen for the plane-wave expansion of eigenfunctions. The generalized gradient approximation of Perdew-Burke-Ernzerhof form was employed for electron exchange and correlation^[40-41]. The Brillouin zone was sampled using a Monkhorst-Pack 3×4×1 k-point mesh and the Methfessel-Paxton smearing with 0.1 eV width^[42]. For each structure, the atomic positions were optimized by Hellman-Feynman forces until all the forces were less than 0.1 eV/nm^[43]. All the calculations were conducted at the spin-polarized state.

The bcc Fe $\Sigma 3(111)$ $[\bar{1}\bar{1}0]$ symmetrical tilt GB was used in calculations and the structural cell including two GBs is shown in Fig.1. The directions of a , b , and c axes are indicated by arrows. Before constructing the α -Fe $\Sigma 3(111)$ symmetrical tilt GB, the lattice parameter of bulk bcc Fe is 0.2833 nm, which is quite similar to other calculated results and experimental results^[44-45]. The model is designed as a sandwich model with two GBs in one cell. Fe atoms in brown color are 0.5 a distance from the Fe atoms in blue color in $\langle \bar{1}\bar{1}0 \rangle$ direction. In this model, the pure α -Fe $\Sigma 3(111)$ GB contains 96 atoms. There are two GB planes in the unit model, both of which are marked by dash lines in Fig. 1a. Fig. 1b shows the top view of the (111) surface at GB plane. The atoms in the clean GB model (without Mg addition) are relaxed into the one with the most stable position before inserting any foreign atoms, and the optimized dimensions of GB were calculated as 0.801 nm×0.694 nm×1.963 nm. The free surface (FS) system (Fig. 1c) is half of GB model with a vacuum layer larger than 1.5 nm, which ensures no significant interactions between the periodic surface slab. The positions of the atoms at GB plane are denoted as site 1, and the atoms located in the layer next to GB are named as site 2 (or site -2), site 3 (or site -3), etc. The substitute sites in the middle layer (site 7) between two GB planes are deemed as the bulk sites. All the possible substitute places (or interstitial sites) in GB model were calculated for energy comparison.

In this research, the segregation ability of these two atoms was firstly analyzed to investigate the effect of Mg on the segregation behavior of P at GB. The segregation energy of the atom M on site n is E_{Mseg}^n , and it is expressed by Eq.(1), as follows:

$$E_{Mseg}^n = E_{MGB}^n - E_{Mbulk} \quad (1)$$

where E_{MGB}^n is the total energy of GB model with one solute atom M at n site and E_{Mbulk} is the total energy of GB model with the solute atom at the bulk site. The negative E_{Mseg}^n value indicates the GB segregation potential, whereas the positive value implies that the bulk site is more popular compared with the segregation position. The embrittlement potency energy of GB with different impurities was also obtained based on the intergranular fracture induced by Rice-Wang thermodynamic theory of segregation^[46-47]. This energy is defined as the difference between the segregation energies of the atom at GB and FS, which can be calculated by Eq.(2), as follows:

$$\Delta E = (E_{GB}^M - E_{GB}) - (E_{FS}^M - E_{FS}) \quad (2)$$

where E_{GB}^M , E_{FS}^M , E_{GB} , and E_{FS} represent the total energies of the atom M segregated GB, atom M segregated FS slabs, clean GB, and clean FS, respectively. The negative or positive value of ΔE implies a strengthening or weakening effect of the atom to GB. The larger the ΔE value, the stronger the effect.

3 Results and Discussion

3.1 Segregation behavior of P and Mg at α -Fe $\Sigma 3(111)$ GB

Firstly, put P and Mg at different segregation sites to find their most popular locations at α -Fe $\Sigma 3(111)$ GB. Herein, five substitution sites are considered, which are site 1, 2, 3, 4, and 5 for both P and Mg, as shown in Fig. 1a. Based on the research results in Ref. [18–19], P is more likely to substitute Fe atom rather than to insert as an interstitial atom, and the atom radius of Mg (approximately 0.16 nm) is also too large to be located at the interstitial site of GB model. The segregation energy of an interstitial Mg atom at GB plane is quite positive as 6.0233 eV/atom, indicating an unstable position. The segregation energies of all these possible location sites are shown in Fig. 2. The insets in Fig. 2 show part of GB system, where the light blue balls are the foreign atoms (P or Mg) when they are located at their most stable segregation sites. Dash lines indicate GB planes. It can be seen that both P and Mg prefer to segregate at GB or near GB zone rather than in the bulk position. The segregation energies

of P at substitution sites 1–5 are all negative. The segregation energy of P at substitution site 4 is negative but only of -0.1 eV, which is very close to zero. These calculation results are in accordance with the results in Ref. [4–5], which emphasized that both P and Mg were found at GB of 2.25Cr-1Mo ferrite steel by AES analysis. Compared with that of P, the segregation tendency of Mg is less strong with a segregation energy of about 1.36 eV, which is higher than that of P. Moreover, it also needs to point out that the most stable segregation sites for P and Mg are also quite different. For P, the most stable position is site 2, which locates at the atom layer next to GB plane; for Mg, the favorable site is site 1, which locates at GB plane.

To clarify different segregation behavior between P and Mg, the atom distance change of GB with different atom solutions was analyzed. Herein, the atom distance deviation d_{dev} is introduced, as follows:

$$d_{dev}^{i-j} = d_M^{i-j} - d_{GB}^{i-j} \quad (3)$$

where d_M^{i-j} is the atom distance between site i and site j in GB model with the solute atom M ; d_{GB}^{i-j} is the distance of site i and site j in clean GB. A negative result of d_{dev} implies an atom distance shrinkage, whereas a positive d_{dev} value indicates a localized expansion, compared with the original distance. The atom distance deviations are shown in Fig. 3 and the atom distances in clean GB are listed in Table 1. It is found that the

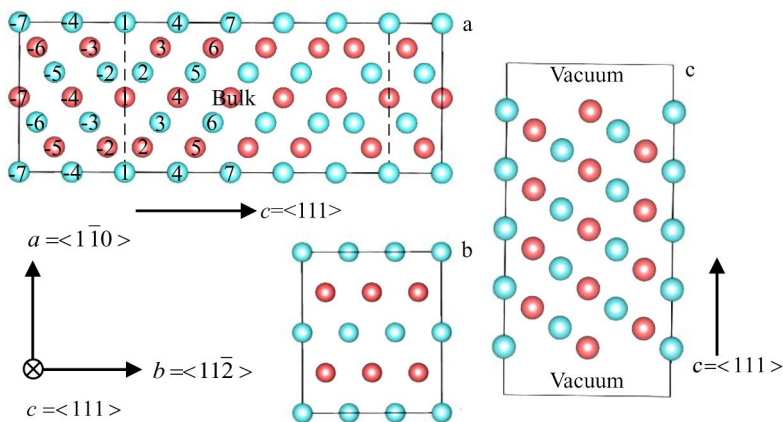


Fig. 1 Structural models of bcc Fe $\Sigma 3(111)$ $[1\bar{1}0]$ symmetrical tilt GB (a–b) and (111) FS system (c): (a) overall model; (b) top view of (111) surface at GB plane

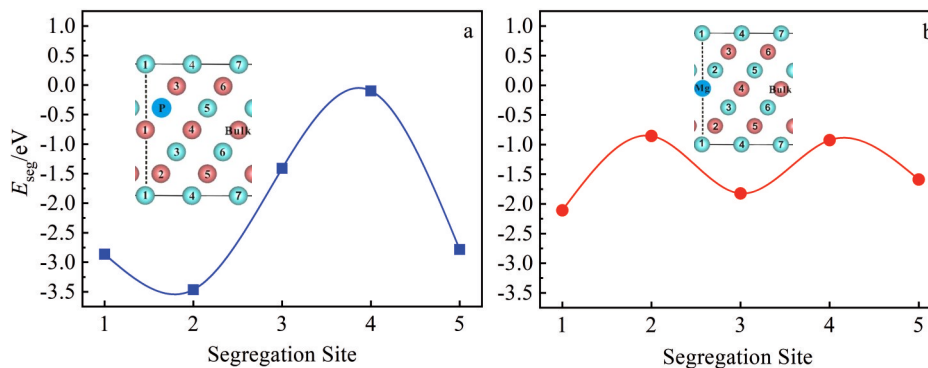


Fig. 2 Calculated segregation energy E_{seg} for P (a) and Mg (b) at different segregation sites in GB system

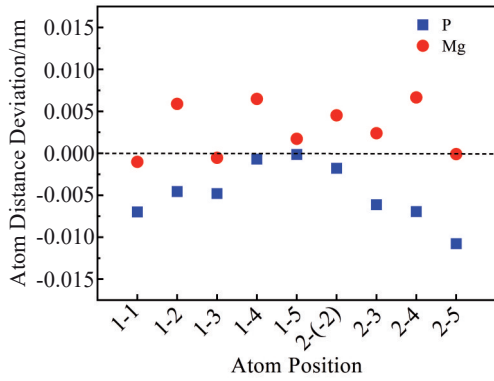


Fig.3 Atom distance deviations in GB model after P and Mg substitution

atom at site 2 usually has shorter distance to surrounding Fe atoms (0.2143–0.2711 nm), whereas the atoms at site 1 have larger space with longer atom distance to their neighbors (0.2549–0.4070 nm). When foreign atoms are segregated, the distances between atoms in GB model change, as shown in Fig.3. It can be seen that when P substitutes the atom at site 2, the atom distances between P and its surrounding Fe atoms are all decreased, which is reflected by the negative distance deviations. The nearest atom to P is a Fe atom at site -2. The distance between these two atoms is 0.2125 nm. The second,

third, and fourth nearest atoms are at site 5, 3, and 1 with the distance of 0.2170, 0.2313, and 0.2504 nm, respectively. When the atom at site 1 is substituted by Mg atom, the atom distance deviations are all positive, indicating a GB zone expansion, which is mainly induced by the lattice distortion when Mg atoms with large radius are inserted.

To specify the reasons of different atom segregation behavior, partial density of states (PDOS) of both P and Mg with its first and second nearest Fe atoms was analyzed, and the results are shown in Fig. 4 and Fig. 5, respectively. According to Fig.4, P has strong interaction with Fe atoms. Compared with Fe atoms in clean GB, obvious hybridization peaks can be observed from -12.0 eV to -11.9 eV. These peaks are mainly formed by the hybridization of s-orbit electrons of P and s-, p-, and d-orbit electrons of Fe. The localized electrons form strong bonds between P and its nearby Fe atoms, thus leading to the preferential location of P as the place with the nearest Fe atoms. The similar results are also reported in Ref.[19].

PDOS of Mg is shown in Fig. 5. Different from P, no significant hybridization peaks can be found between Mg and its surrounding Fe atoms. There are interactions between the s- and p-orbit electrons of Mg and Fe, but the bonding is not very strong. The valence electrons of Mg are much less compared with those of Fe and P atoms, and with Mg atom

Table 1 Atom distances in clean GB model (nm)

$i-j$	1-1	1-2	1-3	1-4	1-5	2-(-2)	2-3	2-4	2-5
d_{GB}^{i-j}	0.4006	0.2549	0.2818	0.2484	0.4070	0.2143	0.2374	0.2711	0.2278

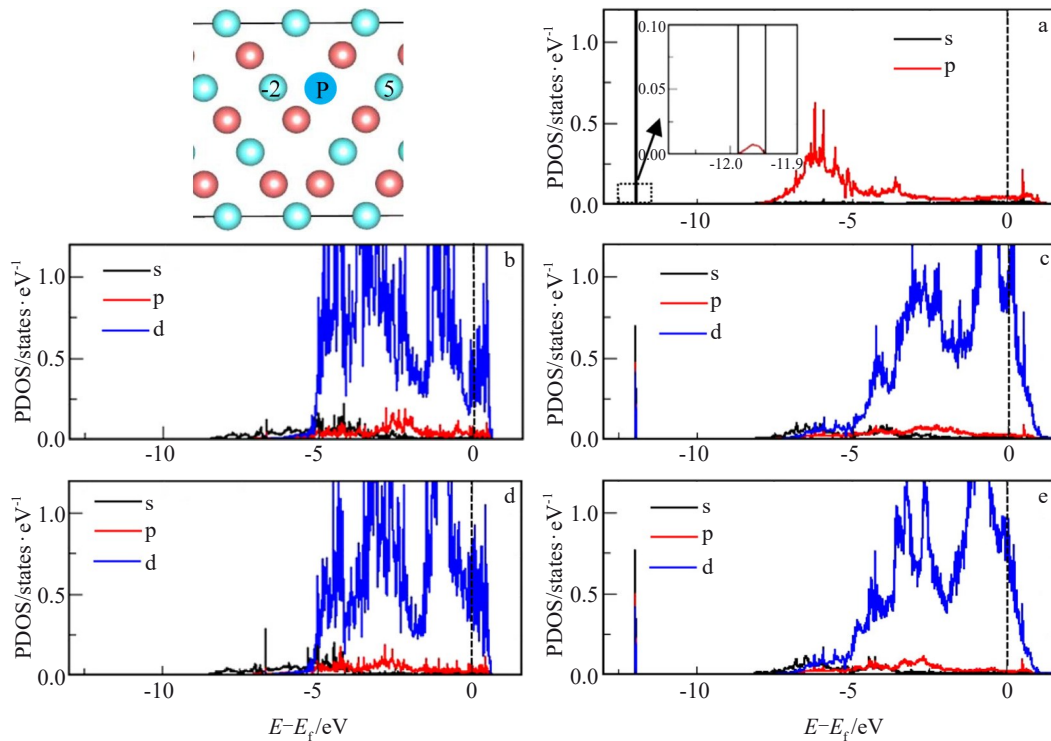


Fig.4 PDOSs of P and Fe atoms: (a) PDOS of P atom; (b) PDOS of Fe atoms at site -2 in clean GB; (c) PDOS of Fe atoms at site -2 in P-containing GB; (d) PDOS of Fe atoms at site 5 in clean GB; (e) PDOS of Fe atoms at site 5 in P-containing GB

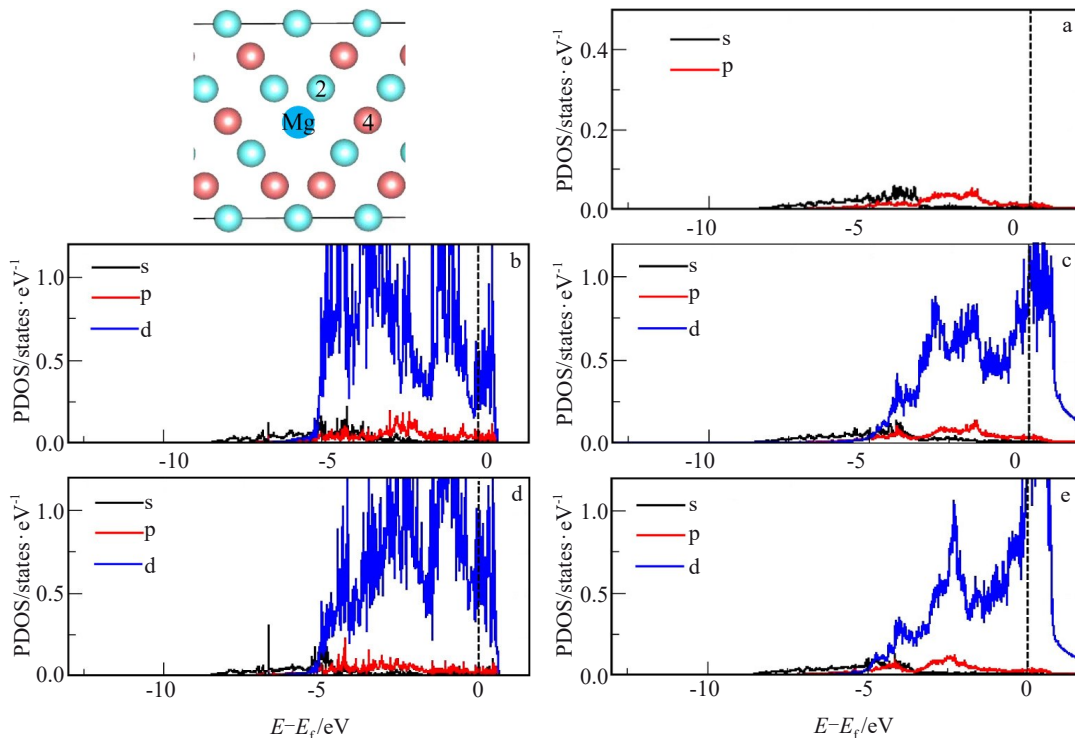


Fig.5 PDOSs of Mg and Fe atoms: (a) PDOS of Mg atom; (b) PDOS of Fe atoms at site 2 in clean GB; (c) PDOS of Fe atoms at site 2 in Mg-containing GB; (d) PDOS of Fe atoms at site 4 in clean GB; (e) PDOS of Fe atoms at site 4 in Mg-containing GB

substitution, the d-orbit electrons of Fe atom are found to decrease, compared with those in clean GB. This infers that Mg addition affects the electron density of states of the surrounding Fe atoms and forms weak bonds with them, which may be a major reason for the reduction in GB strength.

The effects of P and Mg on bcc Fe $\Sigma 3(111)$ GB strength are also analyzed. The embrittlement potency energies of GB with P and Mg are calculated as 0.410 (40 kJ/mol) and 0.730 eV (70 kJ/mol), respectively. The positive values indicate that both P and Mg have a negative effect on GB cohesion, but Mg has a more significant embrittlement potency, compared with P. This result is coincident with the conclusion in Ref. [13]. Lejček et al.^[48] compiled the theoretical values of impurity elements on GB embrittlement. They emphasized that the embrittlement potency calculation is very sensitive to the calculation details, such as the lattice dimension and the relaxation parameters. For instance, the embrittlement potency energy of P had a quite large data range from -89 kJ to 99 kJ under different density functional theory (DFT) calculations. In this theoretical result, the embrittlement potency energy of P (40 kJ/mol) is in the mentioned range and also has a good match with the experimental value in polycrystalline (35–48 kJ)^[46]. The theoretical result for Mg with DFT calculation is lacking, but the result in this research shows a convincing value by considering the embrittlement potency tendency of both Mg and P in experiments.

The segregation behavior and embrittlement potential have great relations to the chemical bond between the solute atom and surrounding Fe atoms. The electron localization function

(ELF) was employed to investigate the types of bonds between the solute atoms and Fe atoms. Generally, ELF value higher than 0.5 indicates ionic or covalent bonds, showing highly localized electrons, whereas ELF value lower than 0.5 is more likely to correspond to metallic bond, showing nonlocal electron gas^[49-51]. The results of ELF of GB with P and Mg segregation under different conditions are shown in Fig. 6 and Fig. 7, where $\Delta n(r)$ describes the electron localization function value. As shown in Fig. 6c, there is a charge accumulation in the middle of P and its nearest Fe atoms. It can be seen that a higher electron density (around 0.3) is found between atoms at the sites 1, 2, and -2. When P substitutes for Fe atom, ELF value is as high as 0.6–0.7 in the middle region between P (site 2) and Fe (site -2) atoms, indicating the formation of a covalent bond. Meanwhile, the electron density among site 2 (or -2), site 1, and other surrounded Fe atoms is all decreased. According to the results in Ref. [52] with quantum mechanical cluster calculations, the elements attract charge from the neighboring metal atoms onto themselves, always showing a strong embrittling behavior, because they remove charge from the original metal-metal bonds, which keep GB together. Thus, the embrittlement potential of P to GB can be explained by the fact that P is prone to bonding with Fe and forming covalent bonds with the nearest Fe atoms as the result of the hybridization of s- and p-orbit electrons. When Mg occupies the site 1 of GB plane, the bonds between Mg and surrounding Fe atoms are still metallic, as shown in Fig. 6d and Fig. 7d. Mg has only two electrons at the outer p-orbit, and its valence electrons are

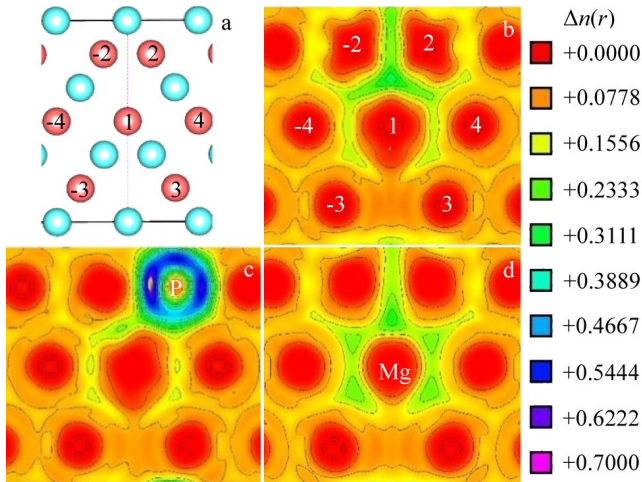


Fig.6 Atomic configuration of $(1\bar{1}0)$ plane, where red atoms are the ones in the same plane and the purple dash line indicates GB plane (a); isosurface of ELF maps and its contour plots: (b) $(1\bar{1}0)$ plane of clean GB; (c) $(1\bar{1}0)$ plane of P-containing GB; (d) $(1\bar{1}0)$ plane of Mg-containing GB

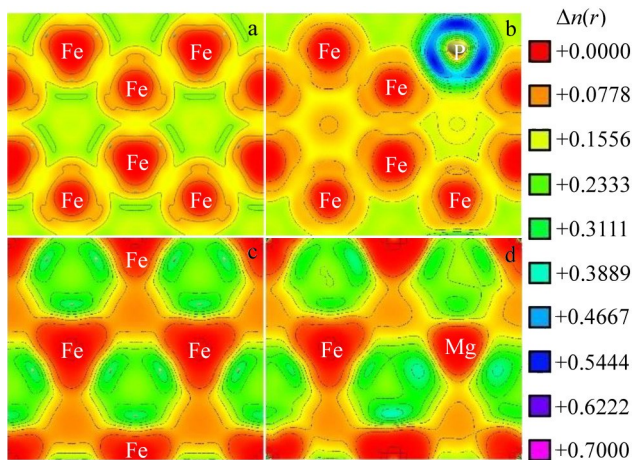


Fig.7 Isosurface of ELF and its contour plots from top view of P substitution plane in clean GB model system (a) and P-containing GB model (b); ELF maps of GB plane in clean GB system (c) and Mg-containing GB (d)

decreased compared with the original Fe atom. Meanwhile, when Mg is inserted in GB plane, the distances between Mg and the surrounding atoms are all increased, which also makes the electron density between Mg and Fe atoms decrease. Less electron density metallic bonds are believed to have lower strength, compared with the previous Fe-Fe bonds, therefore showing an embrittlement behavior when Mg is inserted. Thus, it can be found that the mechanisms for GB embrittlement by P and Mg are quite different. For metalloid atom P, it is more likely to form covalent bonds with the surrounding Fe atoms and to weaken the original Fe-Fe bonds. For metallic atom Mg, GB weakness is more likely induced by two reasons: one is the local strain induced by the oversize

atom insert, which in turn leads to the Fe-Fe atom decohesion; another reason is that Mg has less electrons to form stronger metallic bonds^[14]. To reduce the solution energy, Mg is always prone to substitution for the Fe atom with larger location space and thus more favorable to occupy site 1 with the largest substitution place.

3.2 Effect of Mg on segregation behavior of P at GB

P is seriously detrimental to GB strength and is believed to be the main reason of the temper embrittlement. It is reported that with the addition of a small amount of Mg, the temper embrittlement induced by P can be alleviated to some extent^[4-5]. Mg is known as GB-embitter, which has also been confirmed in this calculation. Herein, with the assistance of theoretical calculation, the effect of Mg on the segregation behavior of P at GB was analyzed. Firstly, the segregation energies of P at the sites 1–5 of Mg-containing GB were calculated. Then, the results of the segregation energies of P at the clean GB were also compiled. All results are shown in Fig. 8. It can be seen that with Mg atom addition, the segregation energies of P are greatly increased. In the clean GB system, the segregation energies are all negative at sites 1–5, which indicates substitution possibility. Particularly, sites 2, 1, and 5 are the most popular sites with the segregation energies as low as -3.462 , -2.863 , and -2.785 eV, respectively. In Mg-containing GB system, site 2 is still the most stable segregation site with the segregation energy of -1.363 eV, but this value is higher than that in clean GB system by about 2.099 eV. When Mg is located in GB plane, site 1 is no longer a possible segregation site for P atoms, because the segregation energy for P atom occupying site 1 rises to 3.380 eV, as shown in Fig. 8. This phenomenon indicates that with the addition of Mg, the number of segregated P atoms around α -Fe $\Sigma 3(111)$ GB is greatly reduced by decreasing from five possible sites (sites 1–5) to only two sites (sites 2 and 5). Besides, according to Mclean's equation^[53], GB element concentration has a great relation to the segregation atom energy, which can be expressed by Eq.(4), as follows:

$$C_{\text{GB}} = \frac{C_{\text{bulk}} \exp(-\Delta E_{\text{atom}}^{\text{seg}}/RT)}{1 + C_{\text{bulk}} \exp(-\Delta E_{\text{atom}}^{\text{seg}}/RT)} \quad (4)$$

where $\Delta E_{\text{atom}}^{\text{seg}}$ is the segregation energy; T is the aging

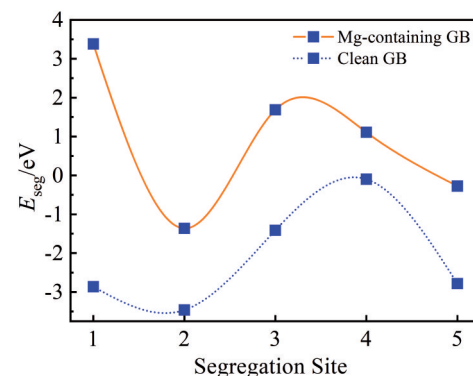


Fig.8 Calculated segregation energy E_{seg} of P at different segregation sites in Mg-containing GB system and clean GB system

temperature; R is the molar gas constant; C_{GB} and C_{bulk} are the impurity occupations of the GB and bulk, respectively. It can be easily identified that with the increase in segregation energy, under the same impurity bulk concentration, the amount of impurity atoms segregating at GB will also be reduced. Thus, it can be reasonably speculated that with the addition of Mg, the segregation of P will be greatly decreased.

To understand the interactions between Mg and P, the electron-distribution around these two atoms was analyzed. Fig. 9 shows ELF maps of P segregated at GB with Mg addition. It can be seen that with the addition of Mg, the covalent bonds between P and the nearest Fe atoms are decreased. Less electrons are accumulated between these two atoms. Moreover, the located electrons are found to drift a little bit from the middle place of site -2 (Fe and P) towards Mg atom, which indicates the possible interaction between Mg and P. According to Fig. 9, it can also be distinguished that

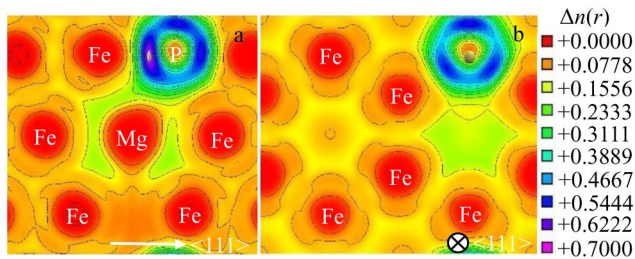


Fig. 9 Isosurface of ELF and its contour plots of atoms around GB plane (a) and top view of atoms at (111) interface (b)

the electron density in the interstitial place around P increases.

PDOS of P, Mg, and their nearest Fe atoms is shown in Fig. 10 to identify the atom interactions when both P and Mg atoms are segregated around GB. Compared Fig. 10a–10b with Fig. 4a and Fig. 5a, it is found that Mg and P have obvious interactions: sharp hybridization peaks can be observed from -12.2 eV to -12.1 eV. This peak is the result of strong hybridization between s-orbit electrons of P and s- and p-orbit electrons of Mg. It should be noticed that the hybridization peak is shifted a little bit to the lower energy place, compared with the original peak in Fig. 4a. This phenomenon indicates a more stable solution behavior when P co-solutes with Mg. Besides, strong interactions are also found between the p-orbit electrons of P and s- and p-orbit electrons of Mg from -8 eV to -3 eV, as shown in Fig. 10a and 10b. These PDOS results indicate that Mg has a stronger interaction with P than with Fe. Meanwhile, the anti-band states in PDOS of P and Fe in Fig. 4 disappear, as shown in Fig. 10, indicating that the bonds between P and Fe decrease. PDOS results have good agreement with the electron density in ELF maps (Fig. 9), suggesting that with the addition of Mg, the interactions are stronger between Mg and P, compared with those between Mg and Fe. All these results indicate that the interaction between Mg and P may reduce the interaction between P and Fe, which is believed to be the major reason causing GB embrittlement.

Moreover, the embrittlement potency energies of GB with both P and Mg were calculated by Eq. (2). It is found that when Mg and P co-segregated at GB, the embrittlement potency energy of GB is around 0.567 eV. This means that the

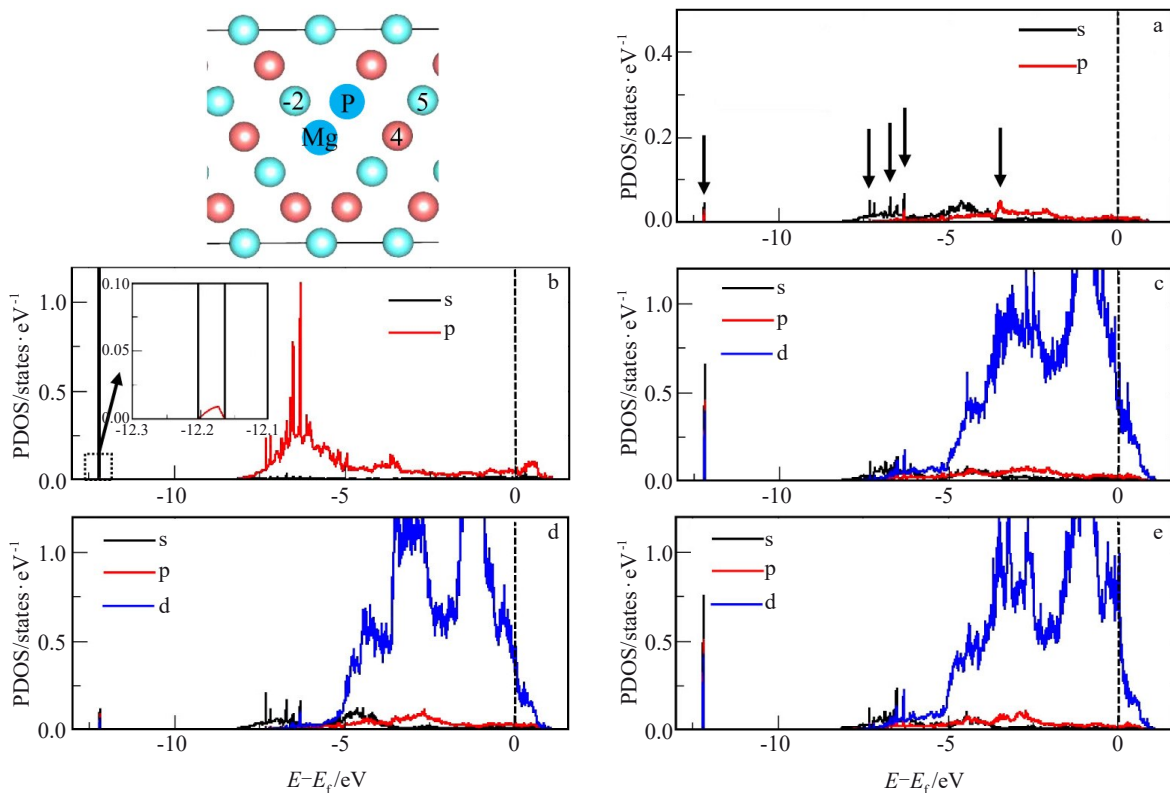


Fig. 10 PDOS of Mg (a), P (b), and Fe (c) at -2 site; PDOS of Fe at site 4 (d) and site 5 (e) in GB model with substituted P and Mg atoms

co-segregation of Mg and P with atom ratio of 1:1 at GB experiences a higher embrittlement potency energy, compared with the state with sole P atom addition. But the energy is much smaller than that of GB with sole Mg atom addition. The great reduction is believed to be caused by the strong interactions between Mg and P. Although the embrittlement potency energy of co-segregation of Mg and P is higher than that with sole P atom in this research, this may be because the ratio of the impurity atoms P and Mg used for calculation is quite higher than that in the experimental case^[4]. Besides, the experimental results indicate that with the addition of 0.056wt% P and 0.005wt%–0.006wt% Mg (atom ratio of Mg and P is about 1:10), the temper embrittlement will be greatly reduced; but when the content of P decreases to 0.002wt% and the amount of Mg addition is fixed (atom ratio of Mg and P is about 3:1), GB strength will be weakened. Thus, it can be concluded that when the content of P is low, the amount of Mg addition may also have an adverse effect on GB strength.

4 Conclusions

1) Both P and Mg are prone to segregation at GB sites. Compared with Mg, P has even stronger segregation potency.

2) The popular sites for P and Mg at GB are different. Mg prefers to occupy the location at GB plane with the largest solution space, whereas P prefers to occupy the sites with the nearest Fe atoms to form strong covalent Fe-P bonds.

3) P and Mg are both embitters to GB of Fe. For metalloid atom P, it is more likely to form covalent bonds with the surrounding Fe atoms and to weaken the original Fe-Fe bonds. For metallic atom Mg, it is more likely induced by two reasons: one is the local strain induced by the oversize atom insert, which in turn leads to the Fe-Fe atom decohesion; the other reason is that Mg has less electrons to form stronger metallic bonds.

4) When GB contains Mg, the segregation behavior of P may be greatly inhibited, due to the decreased possible sites and the increased segregation energy. In this GB system, P has stronger interactions with Mg, showing a lower energy hybridization peak. Therefore, when a small amount of Mg is doped, the temper embrittlement can be moderately inhibited.

References

- Yuan Z X, Song S H, Faulkner R G et al. *Acta Metallurgica et Materialia*[J], 1994, 42(1): 127
- Li Q F, Li L, Liu E B et al. *Scripta Materialia*[J], 2005, 53: 309
- Park S G, Lee K H, Kim M C et al. *Materials Science & Engineering A: Structural Materials: Properties, Microstructure and Processing*[J], 2013, 561: 277
- Li X B, Dong X, Zhao P X et al. *Journal of Iron and Steel Research International*[J], 2021, 28(10): 1259
- Dong X, Li X B, Xing W W et al. *Metals*[J], 2021, 11(1): 10
- Zhang Yuhan, Jin Na, Liu Ying. *Rare Metal Materials and Engineering*[J], 2023, 52(11): 3748
- Li Yuan, Yang Zhong, Duan Hongbo et al. *Rare Metal Materials and Engineering*[J], 2024, 53(1): 95 (in Chinese)
- Wang Pengjia, Li Xiaobing, Peng Baoying et al. *Rare Metal Materials and Engineering*[J], 2024, 53(9): 2513 (in Chinese)
- McMahon C J, Marchut L. *Journal of Vacuum Science and Technology*[J], 1978, 15(2): 450
- Song S H, Zhuang H, Wu J et al. *Materials Science & Engineering A: Structural Materials: Properties, Microstructure and Processing*[J], 2008, 486: 433
- Kameda J, Nishiyama Y. *Materials Science & Engineering A: Structural Materials: Properties, Microstructure and Processing*[J], 2011, 528: 3705
- Guttman M. *Surface Science*[J], 1975, 53(1): 213
- Seah M P. *Acta Metallurgica*[J], 1980, 28(7): 955
- Gibson M A, Schuh C A. *Scripta Materialia*[J], 2015, 113: 55
- Bauer K D, Todorova M, Hingerl K et al. *Acta Materialia*[J], 2015, 90: 69
- Hojna A, Gabirele F D, Klecka J. *Journal of Nuclear Materials*[J], 2016, 472: 163
- Chellali M R, Zheng L, Schlesiger R et al. *Acta Materialia*[J], 2016, 13: 754
- Yamaguchi M, Nishiyama Y, Kaburaki H. *Physical Review B*[J], 2007, 76(3): 035418
- Yuasa M, Mabuchi M. *Physical Review B*[J], 2010, 82(9): 094108
- Grabke H J. *Journal of Steel Research International*[J], 1987, 58(5): 477
- Zheng L, Fu Y, Lejček P et al. *Advanced Engineering Materials*[J], 2016, 18(4): 506
- Wu R, Freeman A J, Olson G B. *Science*[J], 1994, 265(5170): 376
- Wu Chengjian, Tang Xiaoli. *Iron and Steel*[J], 1991, 26(12): 31 (in Chinese)
- Lu Z, Faulkner R G, Sakaguchi N et al. *Journal of Nuclear Materials*[J], 2004, 329: 1017
- Yu J, McMahon C J. *Metallurgical and Materials Transactions A: Physical Metallurgy and Materials Science*[J], 1980, 11: 277
- Song S H, Guo A M, Shen D D et al. *Materials Science & Engineering A: Structural Materials: Properties, Microstructure and Processing*[J], 2003, 360: 96
- Hong S, Lee J, Park K S et al. *Materials Science & Engineering A: Structural Materials: Properties, Microstructure and Processing*[J], 2014, 589: 165
- Heo N H, Jung Y C, Lee J K et al. *Scripta Materialia*[J], 2008, 59: 1200
- Holzmann M, Vlach B, Man J. *Scripta Materialia*[J], 1992, 26: 615
- Saxena S K. *1996 Steelmaking Conference Proceeding*[C]. Pittsburgh: Iron and Steel Society, 1996: 89
- Ohta H, Suito H. *Metallurgical and Materials Transactions B: Process Metallurgy and Materials Processing Science*[J], 1997, 28: 1131

- 32 Yang J, Okumura K, Kuwabara M et al. *Metallurgical and Materials Transactions B: Process Metallurgy and Materials Processing Science*[J], 2003, 34: 619
- 33 Li X B, Min Y, Liu C J et al. *Journal of Steel Research International*[J], 2016, 23(5): 415
- 34 Li Xiaobing, Zhang Tongsheng, Min Yi et al. *Ironmaking & Steelmaking*[J], 2019, 46(3): 301 (in Chinese)
- 35 Kresse G, Hafner J. *Physical Review B*[J], 1993, 48(17): 13115
- 36 Kresse G, Furthmüller J. *Computational Materials Science*[J], 1996, 6(1): 15
- 37 Kresse G, Furthmüller J. *Physical Review B*[J], 1996, 54(16): 11169
- 38 Blöchl P E. *Physical Review B*[J], 1994, 50(3): 1759
- 39 Kresse G, Joubert D. *Physical Review B*[J], 1999, 59(3): 1758
- 40 Perdew J P, Burke K, Ernzerhof M. *Physical Review Letters*[J], 1996, 77(18): 3865
- 41 Hammer B, Hansen L B, Nørskov J K. *Physical Review B*[J], 1999, 59(11): 7413
- 42 Monkhorst H J, Pack J D. *Physical Review B*[J], 1976, 13(12): 5188
- 43 Feynman R P. *Physical Review B*[J], 1939, 56(1): 340
- 44 Pascuet M I, Bonny G, Monnet G et al. *Journal of Nuclear Materials*[J], 2020, 539: 152319
- 45 He Y, Li Y J, Chen C F et al. *International Journal of Hydrogen Energy*[J], 2017, 42: 27438
- 46 Rice J R, Wang J S. *Materials Science & Engineering A: Structural Materials: Properties, Microstructure and Processing*[J], 1989, 107: 23
- 47 Liu W G, Han H, Ren C L et al. *Computational Materials Science*[J], 2014, 88: 22
- 48 Lejček P, Šob M, Paidar V. *Progress in Materials Science*[J], 2017, 87: 83
- 49 Xiao Z, He L, Bai X M. *Journal of Alloys and Compounds*[J], 2021, 874: 159795
- 50 Becke A D, Edgecombe K E. *Journal of Chemical Physics*[J], 1990, 92: 5397
- 51 Silvi B, Savin A. *Nature*[J], 1994, 371(6499): 683
- 52 Messmer R P, Briant C L. *Acta Materialia*[J], 1982, 30: 457
- 53 Mclean D. *Grain Boundaries in Metals*[M]. Oxford: Clarendon Press, 1957

Mg对 α -Fe $\Sigma 3(111)$ 晶界P偏聚的影响

王鹏家¹, 马宇宁¹, 彭宝营¹, 林 鲲³, 李小兵², 刘 奎²

(1. 北京信息科技大学 机电工程学院, 北京 102206)

(2. 季华实验室, 广东 佛山 528200)

(3. 北京科技大学 固体化学研究所, 北京 100083)

摘要: 采用第一性原理计算方法揭示 α -Fe $\Sigma 3(111)[1\bar{1}0]$ 晶界处P和Mg的偏聚行为以及二者的交互作用。结果表明, P和Mg均会在晶界处偏聚, 且P具有更强的晶界偏聚倾向。Mg倾向于优先在具有最大可吸收空位的晶界平面上发生替换, 而P则倾向于占据靠近铁原子的位置, 促进强共价型Fe-P键的形成。当晶界上有Mg时, P的偏聚行为可能会因可用溶解位点的减少和偏聚能量的增加而显著受阻。在晶界上, P与Mg的相互作用增强, 形成较低能量的混合峰。以上发现阐明了少量Mg的引入如何缓解回火脆化现象。

关键词: α -Fe; 晶界; P; Mg; 偏聚; 密度泛函理论

作者简介: 王鹏家, 男, 1985年生, 博士, 北京信息科技大学机电工程学院, 北京 102206, E-mail: pjwneu@bistu.edu.cn